Optical Thermal Ratchet

L. P. Faucheux, L. S. Bourdieu, P. D. Kaplan, and A. J. Libchaber
NEC Research Institute, 4 Independence Way, Princeton, New Jersey 08540
and Princeton University, Physics Department, Princeton, New Jersey 08544
(Received 31 August 1994)

We present an optical realization of a thermal ratchet. Directed motion of Brownian particles in water is induced by modulating in time a spatially periodic but asymmetric optical potential. The net drift shows a maximum as a function of the modulation period. The experimental results agree with a simple theoretical model based on diffusion.

PACS numbers: 05.40.+j

Let us consider a Brownian particle diffusing in a one-dimensional periodic well-shaped potential. If the potential height is much larger than the thermal noise, the particle is localized in a minimum. Suppose that this potential is asymmetric and characterized by two length scales λ_f and λ_b (forward and backward) and assume that λ_b is larger than λ_f (time $\tau = 0$ in Fig. 1). In an equilibrium situation, not net motion of particles can be induced by a periodic potential, since there is no large scale gradients. However, a time modulation of such a potential, when asymmetric, can induce motion in the following way: Turn the potential off; the particle diffuses freely (time $\tau \leq \tau_{\text{off}}$ in Fig. 1). We call P_f the probability that the particle diffuses forward by more than λ_f during the time τ_{off} (and similarly P_b for the backward probability). Switching the potential on again after a time τ_{off} forces the particle to the forward well with a probability P_f and to the backward one with a probability P_b (time $\tau = \tau_{\text{off}}$ in Fig. 1). We define as $J = P_f - P_b$, the probability current for a particle to advance one step in the periodic potential. Because λ_b is larger than λ_f, P_b is smaller than P_f and the drift is nonzero. As proposed earlier, the time modulation of a periodic asymmetric potential creates directed motion of thermally fluctuating particles [1]. Similar models of engines that extract work from random noise have been recently proposed under the denomination of "thermal ratchets" [2–6]. These models may have some connection with biological motor proteins [7–14].

How does one experimentally realize such a spatially periodic but asymmetric forcing of Brownian particles? One way is to deposit two metallic films on a glass substrate in a periodic but asymmetric fashion, so that applying an ac electric field through these electrodes creates the desired potential for colloidal particles in an aqueous solution. Recent experiments using such a setup confirmed the induced drift [15,16]. However, hydrodynamic interactions and the complicated electrical response of charges in water limited these experiments to only qualitative agreement with theory.

In this Letter, to avoid hydrodynamic interactions we study only one particle (a 1.5 μm diameter polystyrene sphere in room temperature water). To avoid electrolytic effects, the potential is created optically by strongly focusing an infrared laser beam to form an optical tweezer [17,18]. Two oscillating mirrors move the optical trap along a circle at a frequency too high for the particle to feel any net azimuthal force. The radial force, however, does not average to zero, and the particle is confined to diffuse along the circle. We then produce a periodic, asymmetric spatial modulation of the tweezing strength along the circle by synchronizing the rotation of a neutral density filter wheel with the rotation of the optical tweezer. Modulating in time this spatial intensity profile induces a net drift of the Brownian particle. The experiment is in agreement with the theory. We also observe a maximum of the induced motion as a function of the modulation time, related to stochastic resonance [19,20] (see Ref. [21] for an experimental case of resonance using a setup similar to ours). We then discuss the feasibility of particle separation using thermal ratchets.

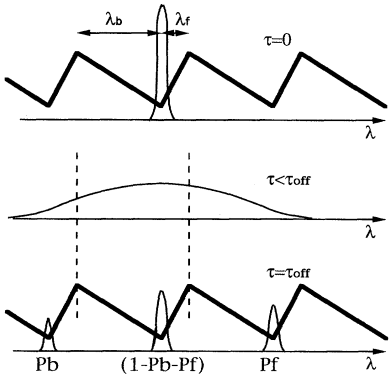

FIG. 1. The asymmetric potential is drawn as the thick line. The forward and backward length scales defining the asymmetry are λ_f and λ_b. The particle probability densities are drawn as thin lines. At time $\tau = 0$, the particle is localized and the probability density is sharply peaked. For times $\tau \leq \tau_{\text{off}}$, the potential is off and the particle diffuses freely. At time $\tau = \tau_{\text{off}}$, the potential is back on and the particle is forced to the forward and backward minimum with probabilities P_f and P_b.

 0031-9007/95/74(9)/1504(4)$06.00

Let us first describe the experimental setup. The samples are prepared by diluting suspensions of 1.5 μm diameter polystyrene spheres in pure water to a volume fraction of 10^{-4}, so that typically only a few beads are seen in the microscope field of view (50×50 μm^2). Mylar sheets of 50 μm thickness are cut and used as spacers between a microscope slide and a coverslip previously cleaned and dried using a nitrogen gas ionizing gun. The cells are then filled with the spheres in suspension and sealed with fast epoxy. The sample, placed on the translation stage of an upright microscope, is observed under bright-field illumination.

The TEM_{00} linearly polarized output of a 1 W power Nd:YAG laser (wavelength = 1064 nm) is inserted into the microscope's optical path via the beam splitter B (see Fig. 2). Strongly focused by a 100× oil coupled objective (OBJ), the beam converges inside the sample to a sharp focal point that acts as an optical trap for the polystyrene sphere. Because of optical losses, the laser power at the sample level is of order 30 mW, and the trapping force is of order a piconewton. Two mirrors $M1$ and $M2$ mounted on galvanometers oscillate around two perpendicular axes with a $\pi/2$ phase difference. Two telescopes $T1$ and $T2$ allow the beam to pivot about the center of the iris diaphragm of the microscope objective as the mirrors oscillate (thus preserving the Gaussian beam profile) [22]. This setup moves the optical trap along a 7 μm diameter circle. A quarter wave plate $\lambda/4$ transforms the linear beam polarization into a circular one: This is necessary to keep the beam intensity constant along the circle. The two galvanometers are synchronously driven at 100 Hz. This frequency is such that the optical tweezer moves too fast for the sphere to follow the trap; the azimuthal force on the particle averages out to zero. The sphere diffuses then freely along the circle *but is still confined in the radial direction.* We checked experimentally that the bead moves diffusively along the circle. We also checked that the trap intensity is constant to within a few percent.

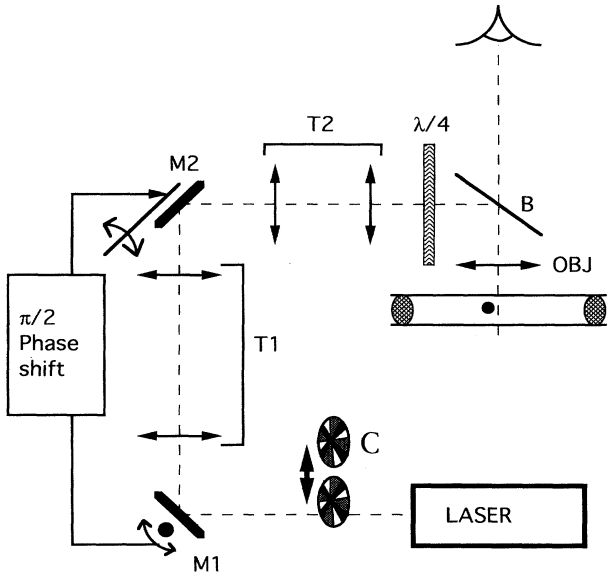

FIG. 2. The sample is observed under bright-field microscopy. The beam splitter B adds the infrared laser beam to the microscope's optical path. The microscope objective OBJ focuses the beam to a focal point, defining an optical trap. Two mirrors $M1$ and $M2$ oscillate around two perpendicular axes with a $\pi/2$ phase difference. They move the trap along a circle (see Fig. 3). Two telescopes $T1$ and $T2$ pivot the beam at the iris diaphragm of the objective OBJ. Circular polarization of the beam is achieved using a quarter wave plate ($\lambda/4$). The filter wheel is mounted on a chopper (C) synchronized with the mirrors. The chopper itself is put on a translation stage which is pulled in and out of the laser path.

We now spatially modulate the beam intensity along the circle in a periodic but asymmetric way. A neutral density filter wheel is mounted on a chopper, the rotation speed of which is synchronized with the rotation of the optical trap (Fig. 2). The shape of the transmission coefficient of the wheel as a function of the rotation angle θ is an asymmetric triangle repeated 4 times as θ goes from 0 to 2π. The maximum attenuation factor is 10^{-2}. Figure 3 shows the beam intensity profile along the circle described by the optical trap. Note that the particle is not trapped and does not rotate at 100 Hz; the spatial modulation localizes, however, the particle in the regions of maximum intensity (see Fig. 3, modulation on). The shape of the effective potential experienced by the sphere along the circle is then indeed an asymmetric triangle characterized by the two length scales λ_f and λ_b shown in Fig. 1. The smaller length scale λ_f is limited by both the laser wavelength and the particle diameter; λ_f is around 2 μm. Experimentally, it takes a few seconds for the particle to fall to the bottom of the potential. Once there, it stays

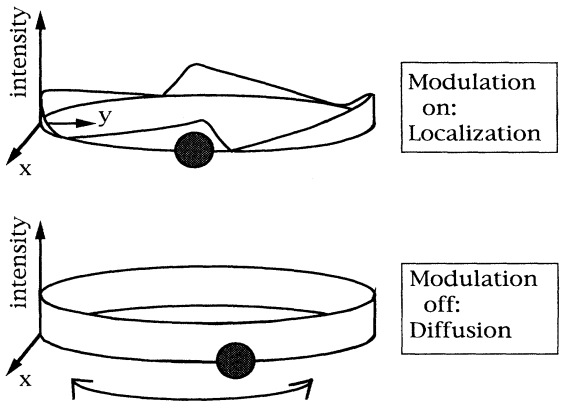

FIG. 3. Modulation on: the spatially asymmetric modulation of the beam intensity along the circle described by the optical trap is shown as the thin solid line (4 modulations per optical trap cycle). The 1.5 μm diameter particle is shown localized in a region of maximum beam intensity. Modulation off: the beam intensity is constant along the circle. The particle diffuses freely in one dimension.

localized: The height of the potential is much larger than the thermal noise k_BT.

We now modulate the beam intensity in time. The chopper is mounted on a translation stage. We manually pull the chopper in and out of the laser path in order to switch on and off the asymmetric spatial modulation of the potential along the circle. When on, the particle gets azimuthally localized in a potential minimum (time $\tau = 0$ in Fig. 1, modulation on in Fig. 3). When off, the particle is still confined on the circle but now diffuses freely along it (time $\tau \leq \tau_{\text{off}}$ in Fig. 1, modulation off in Fig. 3). Turning the spatial asymmetry on again after a time τ_{off} localizes the particle to the minimum where the local gradient of light leads to (time $\tau = \tau_{\text{off}}$ in Fig. 1, modulation on in Fig. 3). The experimental time scales are small enough that the particle does not diffuse by more than the spatial extent of one well. The uncertainty in τ_{off} is of order 1 s. We repeat this experiment N times (N is of order 80) for different τ_{off} and count the total number of forward (N_f) and backward (N_b) bead motions. The forward probability is $P_f = N_f/N$ and the backward one $P_b = N_b/N$. In Fig. 4, the measured probabilities P_f and P_b are plotted as a function of τ_{off}. The vertical error bars on P_f (P_b) represent the statistical uncertainty $\sqrt{N_f}/N$ ($\sqrt{N_b}/N$). As expected for small τ_{off}, the particle does not have enough time to diffuse to the next minimum and stays in the same well; both probabilities tend to zero. For large τ_{off} the particle diffuses to the forward or backward minimum with equal probability 1/2. (This assumes that the particle does not diffuse by more than the spatial extension of one well, which is the case for the range of experimental time scales, it is a short time scale approximation.) The forward probability P_f is then given by [23]

$$P_f = \frac{1}{2}\,\text{Erfc}\left[\frac{\lambda_f}{\sqrt{4D\tau_{\text{off}}}}\right] = \frac{1}{2}\,\text{Erfc}\left[\sqrt{\frac{\tau_f}{2\tau_{\text{off}}}}\right], \quad (1)$$

where Erfc is the complement of the error function and τ_f the average time for the particle to diffuse a distance λ_f, $\tau_f = \lambda_f^2/2D$. D is the diffusion coefficient of a 1.5 μm diameter sphere in water at room temperature ($D = 0.3\ \mu\text{m}^2/\text{s}$). This estimate agrees with the value we find by observing the bead diffusion along the circle when the modulation is switched off. We approximate Eq. (1) by [16,23]

$$P_f = \frac{1}{2}\exp(-\tau_f/\tau_{\text{off}}). \quad (2a)$$

In a similar way the backward probability is approximated by

$$P_b = \frac{1}{2}\exp(-\tau_b/\tau_{\text{off}}), \quad (2b)$$

where the characteristic time τ_b is equal to $\tau_b = \lambda_b^2/2D$. The solid lines in Fig. 4 are fitted to the experimental points using the simple exponentials (2a) and (2b). The results are $\tau_f = 5.3 \pm 0.3$ s and $\tau_b = 12.8 \pm 0.5$ s. From these times we estimate the two length scales, $\lambda_f = 1.8 \pm 0.2\ \mu$m and $\lambda_b = 2.8 \pm 0.2\ \mu$m. The forward characteristic length scale λ_f is close to the bead diameter as expected. These estimates agree with direct observation of the fall of a particle into the potential well.

The net drift ($P_f - P_b$) is shown in Fig. 5 as a function of τ_{off}. The vertical error bars represent the statistical uncertainty $\sqrt{N_f + N_b}/N$. The observed drift increases sharply from zero as τ_{off} approaches τ_f (of order 5 s), reaches a maximum for a time $\tau_{\text{max}} = (\tau_b - \tau_f)/\ln[\tau_b/\tau_f]$ of order 8 s, and then decreases slowly back to zero as τ_{off} becomes larger than τ_b (13 s). The solid line in Fig. 5 is the difference of the two fits in Fig. 4. The value of the drift at resonance is quite small (0.15). It could reach as much as 0.5 in the limit of large (τ_b/τ_f).

A particle with a different diffusion coefficient will show a similar curve with different characteristic time scales. This could be used in principle to sort particles according to their sizes [24]. This is, however, rather unpractical in this experiment. The first limitation comes from the broad width of the resonance (Fig. 5). Making it sharper by reducing the difference between τ_f and τ_b will decrease the strength of the resonance. There are no values of τ_f and τ_b that maximize the quality

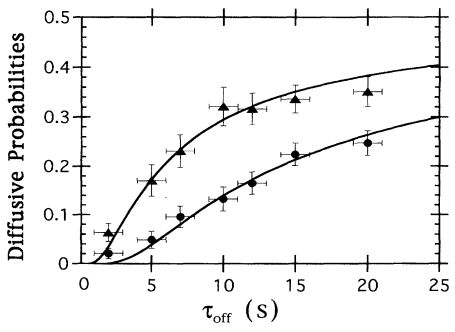

FIG. 4. The probabilities P_f and P_b for a particle to move forward (triangles) and backward (circles) as a function of τ_{off}. The two solid lines are fitted to the data following Eqs. (2a) and (2b).

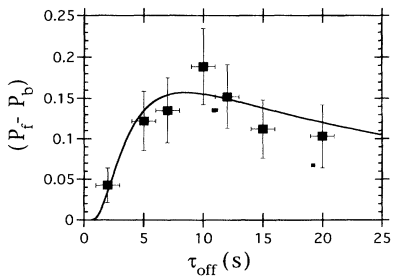

FIG. 5. The probability current ($P_f - P_b$) as a function of τ_{off}. The solid line is the difference between the two fits from Fig. 4.

factor (height over width) of the resonant curve. Another limitation comes from the statistical character of the induced drift: It is only *on average* that the particle motion follows the drift. The on and off switching of the potential then has to be repeated a large enough number of times so that a net particle motion emerges from the diffusive noise.

In conclusion, we have experimentally demonstrated the principle of a thermal ratchet: Broken spatial symmetry and time modulation are indeed enough to induce directed motion from random noise, with a maximum for a characteristic modulation time. Thermal noise can be a tool rather than a physical limit to the efficiency of motors [25].

We gratefully acknowledge the help of A. Ott and A. Schweitzer in designing and building the experimental setup. We thank D. Chatenay, D. Muraki, J. Prost, and M. Shelley for enlightening discussions.

[1] A. Ajdari and J. Prost, C.R. Acad. Sci. Paris **315**, 1635 (1992).
[2] R.P. Feynman, R.B. Leighton, and M. Sands, *The Feynman Lectures in Physics* (Addison-Wesley, Reading, 1966).
[3] J. Prost, J.F. Chauvin, L. Peliti, and A. Ajdari, Phys. Rev. Lett. **72**, 2652 (1994).
[4] M. Magnasco, Phys. Rev. Lett. **71**, 1477 (1993).
[5] C.R. Doering, W. Horsthemke, and J. Riordan, Phys. Rev. Lett. **72**, 2984 (1994).
[6] R.D. Astumian and M. Bier, Phys. Rev. Lett. **72**, 1766 (1994).
[7] B. Alberts, D. Bray, J. Lewis, M. Raff, K. Roberts, and J.D. Watson, *The Molecular Biology of the Cell* (Garland, New York, 1989).
[8] M. Magnasco, Phys. Rev. Lett. **72**, 2656 (1994).
[9] C.S. Peskin, G.M. Odell, and G.F. Oster, Biophys. J. **65**, 316 (1993).
[10] S.M. Simon, C.S. Peskin, and G.F. Oster, Proc. Natl. Acad. Sci. U.S.A. **89**, 3770 (1992).
[11] R. Vale and F. Oosawa, Adv. Biophys. **26**, 97 (1990).
[12] K. Svoboda, C.F. Schmidt, B.J. Schnapp, and S.M. Block, Nature (London) **365**, 721 (1993).
[13] J.T. Finer, R.M. Simmons, and J.A. Spudich, Nature (London) **368**, 113 (1994).
[14] J.M. Scholey, *Motility Assays for Motor Proteins* (Academic, New York, 1993).
[15] S. Leibler, Nature (London) **370**, 412 (1994).
[16] J. Rousselet, L. Salome, A. Ajdari, and J. Prost, Nature (London) **370**, 447 (1994).
[17] A. Ashkin, Phys. Rev. Lett. **24**, 156 (1970).
[18] A. Ashkin, J.M. Dziedic, J.E. Bjorkholm, and S. Chu, Opt. Lett. **11**, 288 (1986).
[19] H.A. Kramers, Physica (Utrecht) **7**, 284 (1940).
[20] R. Benzi, G. Parisi, A. Sutera, and A. Vulpiani, SIAM J. Appl. Math. **43**, 565 (1983).
[21] A. Simon and A. Libchaber, Phys. Rev. Lett. **68**, 3375 (1992).
[22] K. Svoboda and S. Block, A. Rev. Biophys. Biomol. Str. **23**, 247 (1994).
[23] A. Ajdari, Ph.D. thesis, Université Paris 6, Chap. VI.
[24] A. Ajdari and J. Prost, Proc. Natl. Acad. Sci. U.S.A. **88**, 4468 (1991).
[25] H.S. Leff and A.F. Rex, *Maxwell's Demon; Entropy, Information, Computing* (Princeton University Press, Princeton, 1990).